Local Stability of Double-Coped Beams

BO DOWSWELL and ROBERT WHYTE

ABSTRACT

Localized web buckling can limit the strength of coped beams. In this paper, the coped portion of the beam is treated as an isolated rectangular member, and a parametric study is used to develop lateral-torsional buckling modification factors for use with 2010 AISC *Specification* Section F11. The parametric study included finite element models with different cope lengths at the top and bottom flanges and cope depths up to 40% of the beam depth. Compared with the finite element results in this paper, the proposed design procedure is more accurate than the design procedure in the 14th Edition *Steel Construction Manual*.

Keywords: web buckling, coped beams, double copes.

INTRODUCTION

In beam-to-girder connections, the beam is usually coped to allow a standard connection to the girder web. If the beam and girder are of equal nominal depth, both flanges must be coped as shown in Figure 1. The cope length can be large at skewed beam connections; connections to wide flange truss chords; and other, less-common framing conditions. Additionally, it is common for double-coped beams to have unequal cope depths at the top and the bottom, and some connections require unequal cope lengths.

Due to the flexural and shear stresses in the coped portion of the web, web buckling can limit the local strength. The AISC *Steel Construction Manual* (AISC, 2011) provides a design procedure for localized stability of double-coped beams. The equations were developed by Cheng, Yura and Johnson (1984) based on a lateral torsional buckling model with an adjustment factor determined by curve-fitting data from elastic finite element models. Because the adjustment factor was derived using finite element models, limits of applicability were placed on the design equations. One goal of this paper is to expand the finite element database and the limits of applicability of the design equations.

EXISTING PUBLICATIONS

Cheng et al. (1984)

Cheng et al. (1984) developed the design procedure in the AISC *Steel Construction Manual* (AISC, 2011) with the results of 14 elastic finite element models. BASP finite element software was used as described by Akay, Johnson and Will (1977). The models were braced laterally at the face of the compression flange cope. The buckled shapes showed that the tension edge of the coped cross-section experienced lateral movement, and the shear center of the coped region experienced lateral movement and twisting. The design procedure was developed based on a lateral torsional buckling model with an adjustment factor determined by curve-fitting data from the finite element models. All models had maximum cope depths of 20% of the beam depth and equal cope sizes at the top and bottom flanges.

Steel Construction Manual (AISC, 2011)

The model for the design procedure developed by Cheng et al. (1984) is shown in Figure 1. The required flexural strength at the face of the cope is

$$M_r = R_r e \tag{1}$$

The nominal flexural strength is

$$M_n = F_{cr} S_{net} \tag{2}$$

The critical stress is

$$F_{cr} = 0.62\pi E f_d \frac{t_w^2}{ch_0} \le F_y \tag{3}$$

The adjustment factor is

$$f_d = 3.5 - 7.5\left(\frac{d_{ct}}{d}\right) \tag{4}$$

where

E = modulus of elasticity, ksi
F_y = specified minimum yield stress, ksi
R_r = required end reaction, kips

Bo Dowswell, P.E., Ph.D., Principal, ARC International LLC, Birmingham, AL (corresponding). E-mail: bo@arcstructural.com

Robert Whyte, P.E., S.E., Assistant Project Manager, LBYD Inc., Birmingham, AL. E-mail: rwhyte@lbyd.com

S_{net} = section modulus of the coped section, in.^{3}
c = cope length, in.
d = beam depth, in.
d_{ct} = depth of the top cope, in.
e = distance from the face of the cope to the end reaction, in.
h_o = reduced depth of web, in.
t_w = web thickness, in.

The preceding equations are based on a lateral torsional buckling model and are valid when $c \le 2d$ and $d_c \le 0.2d$. If $d_c > 0.2d$, the following equations, which are based on a plate-buckling model (Muir and Thornton, 2004), are applicable.

$$F_{cr} = F_y Q \tag{5}$$

The reduction factor for plate buckling is

when $\lambda \le 0.7$

$$Q = 1.0 \tag{6a}$$

when $0.7 < \lambda \le 1.41$

$$Q = 1.34 - 0.486\lambda \tag{6b}$$

when $\lambda > 1.41$

$$Q = \frac{1.30}{\lambda^2} \tag{6c}$$

The slenderness parameter is

$$\lambda = \frac{h_0}{10t_w}\sqrt{\frac{F_y}{475 + 280\left(\frac{h_0}{c}\right)^2}} \tag{7}$$

Figure 2 shows a plot of the critical stress, F_{cr}, versus h_o/d for $c/d = 1$ and $t_w = 0.3$ in. The critical stress for lateral torsional buckling is calculated with Equations 3 and 4 without the yield stress limit. The critical stress for local buckling is calculated with Equations 5, 6 and 7. It can be seen that the two curves are trending in opposite directions, with F_{cr} increasing with h_o/d for lateral torsional buckling and decreasing with h_o/d for local buckling. This indicates the need for a single, continuous function that covers the entire range of applicability.

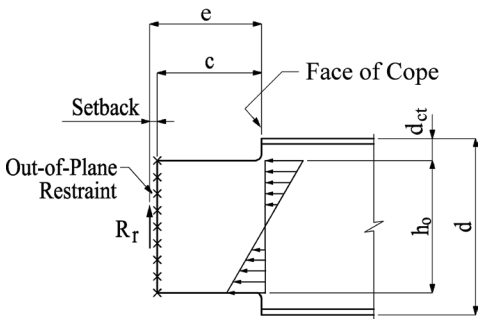

Fig. 1. Double-coped beam.

AISC *Specification* Section F11

Because the *Manual* equations developed by Cheng et al. (1984) were based on a lateral torsional buckling model, AISC *Specification* (AISC, 2010) Section F11 will be reviewed here. Section F11 provides design information for the flexural strength and stability of rectangular members bent about their major axis.

For yielding, $\frac{L_b d}{t^2} \le \frac{0.08E}{F_y}$

$$M_n = M_p = F_y Z \le 1.6M_y \tag{8}$$

For inelastic lateral torsional buckling, $\frac{0.08E}{F_y} < \frac{L_b d}{t^2} \le \frac{1.9E}{F_y}$

$$M_n = C_b\left[1.52 - 0.274\left(\frac{L_b d}{t^2}\right)\frac{F_y}{E}\right]M_y \le M_p \tag{9}$$

For elastic lateral torsional buckling, $\frac{L_b d}{t^2} > \frac{1.9E}{F_y}$

$$M_n = F_{cr} S_x \le M_p \tag{10}$$

The critical stress is

$$F_{cr} = \frac{1.9EC_b}{\frac{L_b d}{t^2}} \tag{11}$$

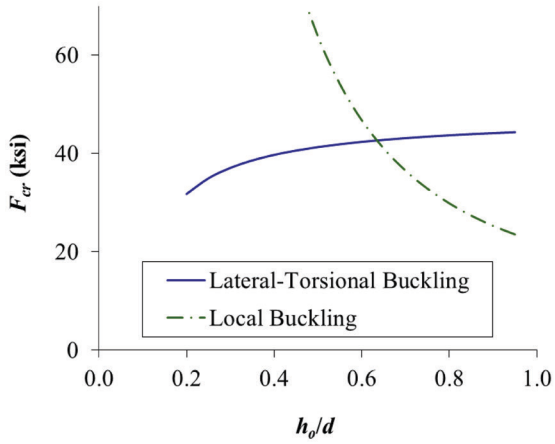

Fig. 2. Critical stress versus h_o/d.

where

C_b = lateral torsional buckling modification factor
L_b = distance between brace points, in.
M_n = nominal moment, kip-in.
M_y = yield moment, kip-in.
M_p = plastic moment, kip-in.
S_x = elastic section modulus, in.^{3}
Z = plastic modulus, in.^{3}
t = beam width, in.

Equation 11 is the theoretical solution for lateral torsional buckling (Timoshenko and Gere, 1961) multiplied by C_b and simplified by substituting the properties for a rectangular cross-section. It can be shown that Equation 3 is equal to Equation 11 by substituting $t = t_w$, $d = h_0$, $L_b = c$ and $C_b = f_d$ into Equation 11. Therefore, f_d is simply a lateral torsional buckling modification factor applied to the theoretical equation for the critical moment of a rectangular beam.

FINITE ELEMENT MODELS

AISC *Specification* Section F2 equations for lateral torsional buckling of wide flange beams are based on the theoretical solution (Timoshenko and Gere, 1961), with C_b factors developed primarily using elastic finite element models. The inelastic portion of the buckling curve was developed by mapping, based on limited testing and finite element results in the inelastic zone. Because much of the inelastic research was based on a constant moment along the beam length (C_b = 1), the full beam length was inelastic. Therefore, the buckling curves are conservative for $C_b > 1$ because they don't account for partial inelasticity along the beam. This same procedure was used in this research to develop equations for the local stability of coped beams.

The finite element program was designed to address three issues related to the local stability of double-coped beams:

1. Cope depths greater than 20% of the beam depth.
2. Unequal cope depths at the top and bottom.
3. Unequal cope lengths at the top and bottom.

A parametric study consisting of 54 elastic, finite element models was used to determine the effect of each variable on the critical load. Using the variables shown in Figure 3, the program consisted of 30 models with $c_t = c_b$, 12 models with $c_t > c_b$, and 12 models with $c_t < c_b$. The details are listed in Appendix A, Tables A1, A2 and A3, respectively.

All models were built with the nominal dimensions of a W16×26. Models for additional beam sizes are not required because the critical moment is proportional to t_w^3 for beams with identical proportions on the cope geometry. Following the modeling techniques of Cheng et al. (1984), BASP finite element software was used to determine the critical loads, assuming the flanges were laterally braced at the face of the cope. There was no setback dimension in the models; therefore, $c_t = e_t$ and $c_b = e_b$.

RESULTS

Accuracy of Manual Equations

For the models with equal cope lengths at the top and bottom flanges, Table A1 in Appendix A compares the finite element results to the current design procedure in the AISC *Manual* (AISC, 2011). Column 6 lists the critical reactions from the finite element models, R_{fe}, and column 7 lists the critical reactions from AISC *Manual* equations, R_{ce}. Models 1, 2, 5, 6, 11, 12, 15 and 16 had $d_c \le 0.2d$; therefore, R_{ce} was calculated with Equations 1 through 4. For the remaining specimens, R_{ce} was calculated with Equations 5, 6 and 7. The average R_{fe}/R_{ce} ratio, listed in column 10, is 1.54 with a standard deviation of 0.496.

Design Model

All of the finite element models buckled in a similar manner, as shown in Figure 4. Confirming the results of Cheng et al. (1984), the tension edge of the coped cross-section experienced lateral translation, and the shear center experienced lateral translation and twisting. The compression edge of the coped section buckled in the shape of a half sine wave, which extended partially into the uncoped portion of the beam due to lateral translation at the reentrant corner of the cope.

To form a design model, the buckling mode must be identified. The buckled shapes have the appearance of several independent modes, including local buckling, lateral torsional buckling, shear buckling, and distortional buckling.

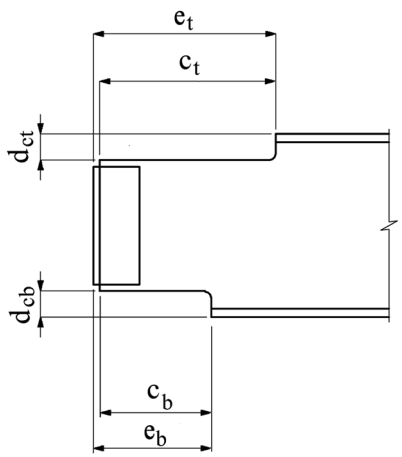

Fig. 3. Different cope sizes at the top and bottom flanges.

The dominant buckling mode is dependent on the cope geometry. Short copes are controlled by shear buckling, and long copes are controlled by lateral torsional buckling, with some aspects of local buckling and distortional buckling present in all cope geometries. Because the buckled shapes most closely resemble lateral torsional buckling over the critical variable range, the design model is based on Equation 11, with the buckling modification factor, C_b, accounting for contributions from the other buckling modes. Factor C_b was determined by curve-fitting the finite element data.

Curve-Fit Equations

The required flexural strength at the face of the cope is

$$M_r = R_r e_{min} \tag{12}$$

The nominal moment is calculated with Equations 10 and 11 with $t = t_w$ and $d = h_0$. The equation for C_b is dependent on the c_t/c_b ratio. For beams with $c_t = c_b$, C_b is calculated using Equation 13 with $L_b = c_t = c_b$. For beams with $c_t < c_b$, C_b is calculated using Equation 13 with $L_b = 0.9c_t + 0.1c_b$.

$$C_b = \left[3.3 + 0.85\sqrt{\frac{d}{L_b}}\ln\left(\frac{L_b}{d}\right)\right]\left[1 - \frac{d_{ct}}{d} + \left(\frac{d_{ct}}{d}\right)^2\right] \tag{13}$$

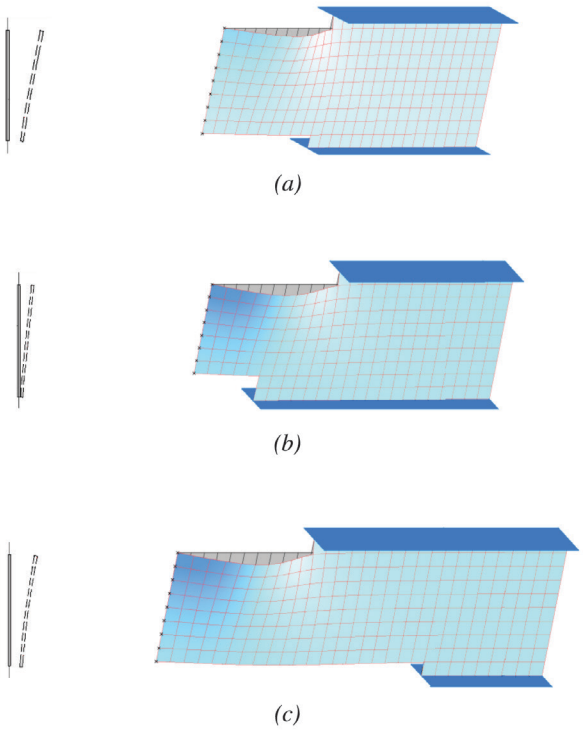

Fig. 4. Buckled shapes: (a) $c_t = c_b$; (b) $c_t > c_b$; (c) $c_t < c_b$.

For beams with $c_t > c_b$, C_b is calculated using Equation 14 with $L_b = (c_t + c_b)/2$.

$$C_b = \left(\frac{c_b}{c_t}\right)\left[3.3 + 0.85\sqrt{\frac{d}{L_b}}\ln\left(\frac{L_b}{d}\right)\right]\left[1 - \frac{d_{ct}}{d} + \left(\frac{d_{ct}}{d}\right)^2\right] \tag{14}$$

where

c_b = length of bottom cope, in.
c_t = length of top cope, in.
d_{cb} = depth of bottom cope, in.
d_{ct} = depth of top cope, in.
e_b = distance from the face of the bottom cope to the end reaction, in.
e_t = distance from the face of the top cope to the end reaction, in.
e_{min} = minimum of e_t and e_b

The results for all models are listed in Tables A1, A2 and A3 in Appendix A. For beams with $c_t = c_b$, the average, finite element-to-calculated load ratio is 1.01 and the standard deviation is 0.0535. For $c_t < c_b$, the average load ratio is 1.02, and the standard deviation is 0.0902. For $c_t > c_b$, the average load ratio is 1.06, and the standard deviation is 0.0752.

Equation 13 is plotted in Figures 5 and 6 with the finite element results for $c_t = c_b$. Figure 5 shows C_b versus c_t/d for four values of d_{ct}/d. Figure 6 shows C_b versus d_{ct}/d for four values of c_t/d.

DESIGN

Moment-Shear Interaction

The design procedure in the AISC *Manual* (AISC, 2011) uses beam theory as the basis for calculation of the flexural stresses. Because the maximum normal and shear stresses occur at different locations on the cross-section, combining these stresses is not required. However, the design procedure proposed in this paper utilizes the plastic flexural strength. Because the plastic stress distribution requires the maximum shear and normal stresses to act at the same location on the cross-section, the flexural strength is reduced in the presence of shear loading. For short cope lengths, the required shear load can be close to the shear yield strength. To account for the interaction between the flexural and shear loads, a reduction factor can be applied to the plastic moment capacity, M_p. Neal (1961) developed Equation 15 for the plastic capacity of a rectangular member subjected to moment about one axis, axial load and shear.

$$\frac{M_r}{M_p} + \left(\frac{P_r}{P_y}\right)^2 + \frac{\left(\frac{R_r}{V_n}\right)^4}{1 - \left(\frac{P_r}{P_y}\right)^2} \le 1.0 \tag{15}$$

where

P_r = required axial load, kips
P_y = axial yield load, kips
R_r = required shear load, kips
V_n = shear yield strength, = $0.6F_y h_o t_w$, kips

The plastic moment strength, reduced to account for the required shear load is

$$M_{pv} = M_p \left[1 - \left(\frac{R_r}{V_n} \right)^4 \right] \quad (16)$$

Because M_{pv} must be based on the available shear strength rather than the nominal value, Equations 17a and 17b should be used in design:

$$\text{LRFD} \qquad M_{pv} = M_p \left[1 - \left(\frac{R_r}{\phi_v V_n} \right)^4 \right] \quad (17a)$$

$$\text{ASD} \qquad M_{pv} = M_p \left[1 - \left(\frac{\Omega_v R_r}{V_n} \right)^4 \right] \quad (17b)$$

Limits of Applicability

Because the curve-fit equations were derived using finite element models, the range of applicability should be based on the cope geometries studied. The geometry of the tension flange cope has a limited influence on the buckling load; therefore, no limits are required on d_{cb} or c_b. The finite element models were limited to a maximum cope length of

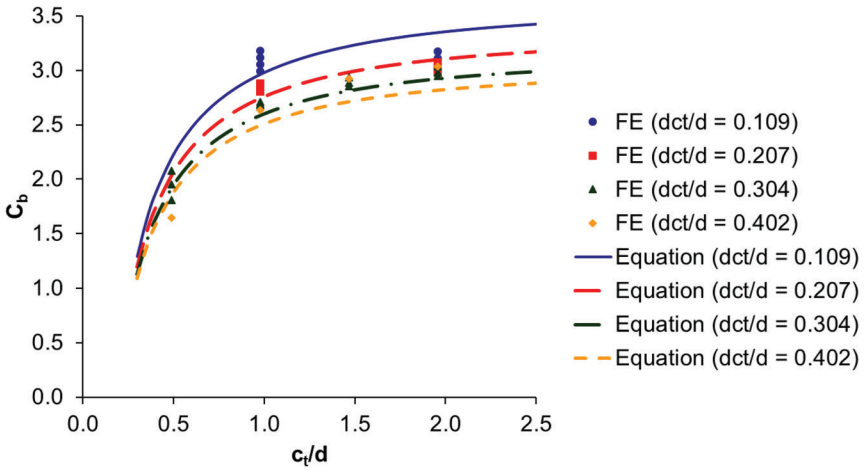

Fig. 5. C_b *versus* c_t/d.

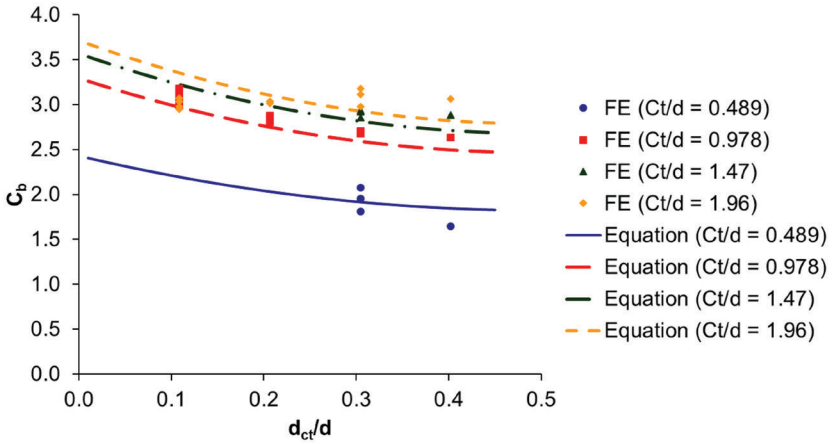

Fig. 6. C_b *versus* d_{ct}/d.

twice the beam depth. Observation of Figure 5 shows that C_b increases slowly for c_t/d greater than 2; therefore, in the rare case that $c_t > 2d$, it is recommended that $c_t = 2d$ is used in the calculations. Because the depth of the compression flange cope was limited to 40% of the beam depth, the equations are valid only for $d_{ct} \le 0.4d$.

When c_t/d is less than 0.5, the curve-fit equations can produce unrealistically low values for C_b. This is because shear buckling dominates the behavior for short copes. To eliminate erroneous calculations, a lower limit can be applied to C_b. According to equations developed by Dowswell (2004), C_b = 1.84 for a rectangular cantilever beam loaded at the shear center with bracing at each end and a concentrated load at the tip. Therefore, a minimum value of C_b = 1.84 is recommended.

Design Proposal

To account for inelastic action, AISC *Specification* Section F11 can be used with $t = t_w$ and $d = h_0$. The following design procedure is suggested:

For yielding, $\lambda \le \lambda_p$:

$$M_n = M_{pv} \tag{18}$$

For inelastic lateral-torsional buckling, $\lambda_p < \lambda \le \lambda_r$:

$$M_n = C_b\left[1.52 - 0.274\lambda\frac{F_y}{E}\right]M_y \le M_{pv} \tag{19}$$

For elastic lateral-torsional buckling, $\lambda > \lambda_r$:

$$M_n = F_{cr}S_x \le M_{pv} \tag{20}$$

The critical stress is

$$F_{cr} = \frac{1.9EC_b}{\lambda} \tag{21}$$

where

$$\lambda = \frac{L_b h_0}{t_w^2} \tag{22}$$

$$\lambda_p = \frac{0.08E}{F_y} \tag{23}$$

$$\lambda_r = \frac{1.9E}{F_y} \tag{24}$$

Simplified Equations

Simplified versions of Equations 13 and 14 can be used for design purposes. For beams with $c_t = c_b$ and beams with $c_t < c_b$, $L_b = c_t$ and C_b is calculated with Equation 25.

$$C_b = \left[3 + \ln\left(\frac{L_b}{d}\right)\right]\left(1 - \frac{d_{ct}}{d}\right) \le 1.84 \tag{25}$$

For beams with $c_t > c_b$, $L_b = (c_t + c_b)/2$ and C_b is calculated with Equation 26.

$$C_b = \left(\frac{c_b}{c_t}\right)\left[3 + \ln\left(\frac{L_b}{d}\right)\right]\left(1 - \frac{d_{ct}}{d}\right) \le 1.84 \tag{26}$$

The simplified equations are compared with the finite element models in Appendix A, Tables A1, A2 and A3. For beams with $c_t = c_b$, the average finite element-to-calculated load ratio is 1.18, and the standard deviation is 0.139. For $c_t < c_b$, the average load ratio is 1.05, and the standard deviation is 0.0736. For $c_t > c_b$, the average load ratio is 1.19, and the standard deviation is 0.0949.

CONCLUSIONS

This paper used the results of a parametric study to formulate a design procedure for the local strength of double-coped beams. Lateral torsional buckling modification factors, for use with AISC *Specification* Section F11, were formulated by curve-fitting the results of 54 finite element models. The proposed solution is based on a larger database of finite element models than the *Manual* procedure, and the limits of applicability have been extended. In contrast to the *Manual* procedure, which has curves trending in opposite directions, the proposed solution provides a single, continuous equation over the entire range of applicability.

The proposed design procedure was shown to be more accurate than the current *Manual* procedure. For beams with equal cope lengths at both flanges, the *Manual* procedure has an average finite element–to–calculated load ratio of 1.54 with a standard deviation of 0.496. The curve-fit equation developed in this paper (Equation 13) produced an average finite element–to–calculated load ratio of 1.01 with a standard deviation of 0.0535. For the simplified equation (Equation 25), the average finite element–to–calculated load ratio is 1.18 with a standard deviation of 0.139.

Using all 54 of the finite element results, calculations using the curve-fit equations (Equations 13 and 14) produced an average finite element–to–calculated load ratio of 1.02 and a standard deviation of 0.0665. The simplified design equations (Equations 25 and 26) had an average finite element–to–calculated load ratio of 1.15 and a standard deviation of 0.115.

ACKNOWLEDGMENTS

The authors would like to thank Professor Joseph Yura at the University of Texas at Austin for providing the finite element program, BASP, used in this study.

SYMBOLS

C_b = lateral torsional buckling modification factor

E = modulus of elasticity, ksi

F_{cr} = critical stress, ksi

F_y = specified minimum yield stress, ksi

L_b = distance between brace points, in.

M_n = nominal moment, kip-in.

M_y = yield moment, kip-in.

M_p = plastic moment, kip-in.

M_{pv} = plastic moment, reduced to account for the required shear load, kip-in.

M_r = required moment, kip-in.

P_r = required axial load, kips

P_y = axial yield load, kips

Q = reduction factor for plate buckling

R_{de} = critical reaction with C_b calculated with the simplified design equation

R_{fe} = critical reaction from finite element model

R_r = required end reaction, kips

R_{re} = critical reaction with C_b calculated with the original regression equation

S_{net} = elastic section modulus of the coped section, in.^{3}

S_x = elastic section modulus, in.^{3}

V_n = shear yield strength, kips

Z = plastic modulus, in.^{3}

c = cope length, in.

c_b = length of bottom cope, in.

c_t = length of top cope, in.

d = beam depth, in.

d_{cb} = depth of bottom cope, in.

d_{ct} = depth of top cope, in.

e = distance from the face of the cope to the end reaction, in.

e_b = distance from the face of the bottom cope to the end reaction, in.

e_t = distance from the face of the top cope to the end reaction, in.

e_{min} = minimum of e_t and e_b

f_d = adjustment factor

h_o = reduced depth of web, in.

t = beam width, in.

t_w = web thickness, in.

Ω_v = safety factor for shear

ϕ_v = resistance factor for shear

λ = slenderness parameter

λ_p = limiting slenderness for the limit state of yielding

λ_r = limiting slenderness for the limit state of inelastic lateral torsional buckling

REFERENCES

AISC (2010), *Specification for Structural Steel Buildings*, American Institute of Steel Construction, Chicago, IL.

AISC (2011), *Steel Construction Manua*l, 14th ed., American Institute of Steel Construction, Chicago, IL.

Akay, H.U., Johnson, C.P. and Will, K.M. (1977), "Lateral and Local Buckling of Beams and Frames," *Journal of the Structural Division,* ASCE, Vol. 103, No. ST9, September, pp. 1821–1832.

Cheng, J.J., Yura, J.A. and Johnson, C.P. (1984), "Design and Behavior of Coped Beam," Ferguson Lab Report, The University of Texas at Austin, July.

Dowswell, B. (2004), "Lateral-Torsional Buckling of Wide Flange Cantilever Beams," *Engineering Journal*, AISC, Second Quarter, Vol. 41, No. 2.

Muir, L.S. and Thornton, W.A. (2004), "A Direct Method for Obtaining the Plate Buckling Coefficient for Double-Coped Beams," *Engineering Journal*, AISC, Third Quarter, Chicago, IL.

Neal, B.G. (1961), "The Effect of Shear and Normal Forces on the Fully Plastic Moment of a Beam of Rectangular Cross Section," *Journal of Applied Mechanics,* Vol. 28, pp. 269–274.

Timoshenko, S. P. and Gere, J. M. (1961), *Theory of Elastic Stability*, 2nd ed., McGraw-Hill, New York.

APPENDIX A. TABLES

Table A1. Finite Element Results with $c_t = c_b$

Model Number	c_t (in.)	c_b (in.)	d_{ct} (in.)	d_{cb} (in.)	R_{fe} (kips)	R_{ce} (kips)	R_{re} (kips)	R_{de} (kips)	$\frac{R_{fe}}{R_{ce}}$	$\frac{R_{fe}}{R_{re}}$	$\frac{R_{fe}}{R_{de}}$
1	15.4	15.4	1.71	1.71	24.4	20.6	22.7	20.3	1.18	1.07	1.20
2	15.4	15.4	3.24	1.71	19.3	13.1	18.4	15.8	1.48	1.05	1.22
3	15.4	15.4	4.78	1.71	15.6	9.35	14.9	11.9	1.66	1.05	1.31
4	15.4	15.4	6.31	1.71	12.6	7.10	11.9	8.53	1.78	1.06	1.48
5	15.4	15.4	1.71	3.24	20.9	18.0	19.9	17.8	1.16	1.05	1.18
6	15.4	15.4	3.24	3.24	16.3	11.2	15.8	13.6	1.46	1.04	1.20
7	15.4	15.4	4.78	3.24	12.9	7.10	12.4	9.92	1.82	1.04	1.30
8	15.4	15.4	1.71	4.78	17.6	9.35	17.0	15.3	1.88	1.03	1.15
9	15.4	15.4	3.24	4.78	13.4	7.10	13.1	11.3	1.89	1.02	1.19
10	15.4	15.4	1.71	6.31	14.3	7.10	14.2	12.7	2.02	1.01	1.13
11	30.7	30.7	1.71	1.71	6.09	5.14	6.42	6.27	1.18	0.948	0.970
12	30.7	30.7	3.24	1.71	5.16	3.27	5.20	4.88	1.58	0.992	1.06
13	30.7	30.7	4.78	1.71	4.36	4.45	4.20	3.67	0.979	1.04	1.19
14	30.7	30.7	6.31	1.71	3.63	3.46	3.37	2.63	1.05	1.08	1.38
15	30.7	30.7	1.71	3.24	5.22	4.50	5.62	5.49	1.16	0.930	0.951
16	30.7	30.7	3.24	3.24	4.34	2.80	4.46	4.19	1.55	0.973	1.04
17	30.7	30.7	4.78	3.24	3.57	3.46	3.50	3.06	1.03	1.02	1.17
18	30.7	30.7	1.71	4.78	4.41	4.45	4.81	4.70	0.989	0.915	0.937
19	30.7	30.7	3.24	4.78	3.57	3.46	3.71	3.49	1.03	0.961	1.02
20	30.7	30.7	1.71	6.31	3.63	3.46	4.01	3.92	1.05	0.906	0.927
21	7.68	7.68	4.78	1.71	41.6	21.0	44.1	36.6	1.98	0.945	1.14
22	7.68	7.68	6.31	1.71	31.5	15.3	35.4	26.2	2.06	0.891	1.20
23	7.68	7.68	4.78	3.24	37.4	15.3	36.7	30.5	2.45	1.02	1.23
24	23.0	23.0	4.78	1.71	7.51	6.02	7.19	6.01	1.25	1.04	1.25
25	23.0	23.0	6.31	1.71	6.22	4.64	5.77	4.31	1.34	1.08	1.44
26	23.0	23.0	4.78	3.24	6.15	4.64	5.99	5.01	1.32	1.03	1.23
27	7.68	7.68	4.78	4.78	31.8	10.2	29.4	24.4	3.11	1.08	1.31
28	15.4	15.4	4.78	4.78	10.3	4.96	9.91	7.94	2.07	1.04	1.29
29	23.0	23.0	4.78	4.78	4.87	3.28	4.79	4.01	1.49	1.02	1.21
30	30.7	30.7	4.78	4.78	2.83	2.45	2.80	2.45	1.15	1.01	1.16
								Average	1.54	1.01	1.18
								Standard Deviation	0.496	0.0535	0.139

R_{fe} = critical reaction from finite element model
R_{ce} = critical reaction from AISC *Manual* equations
R_{re} = critical reaction with C_b calculated with the original regression equation
R_{de} = critical reaction with C_b calculated with the simplified design equation

Table A2. Finite Element Results with $c_t > c_b$									
Model Number	c_t **(in.)**	c_b **(in.)**	d_{ct} **(in.)**	d_{cb} **(in.)**	R_{fe} **(kips)**	R_{re} **(kips)**	R_{de} **(kips)**	$\frac{R_{fe}}{R_{re}}$	$\frac{R_{fe}}{R_{de}}$
32	30.7	15.4	3.24	3.24	6.87	5.72	5.14	1.20	1.33
34	30.7	15.4	1.71	1.71	8.27	8.24	7.71	1.00	1.07
36	30.7	15.4	1.71	3.24	7.69	7.21	6.74	1.07	1.14
38	30.7	15.4	3.24	1.71	7.41	6.67	6.00	1.11	1.23
40	15.4	7.68	3.24	3.24	20.5	19.2	16.4	1.07	1.25
42	15.4	7.68	1.71	1.71	27.9	27.6	24.5	1.01	1.14
44	15.4	7.68	1.71	3.24	25.7	24.2	21.4	1.06	1.20
46	15.4	7.68	3.24	1.71	22.3	22.4	19.1	0.995	1.17
48	30.7	7.68	3.24	3.24	7.94	6.64	5.84	1.19	1.36
50	30.7	7.68	1.71	1.71	9.10	9.57	8.75	0.952	1.04
52	30.7	7.68	1.71	3.24	8.79	8.37	7.65	1.05	1.15
54	30.7	7.68	3.24	1.71	8.25	7.75	6.81	1.06	1.21
							Average	1.06	1.19
							Standard Deviation	0.0752	0.0949

R_{fe} = critical reaction from finite element model
R_{re} = critical reaction with C_b calculated with the original regression equation
R_{de} = critical reaction with C_b calculated with the simplified design equation

Table A3. Finite Element Results with $c_t < c_b$									
Model Number	c_t **(in.)**	c_b **(in.)**	d_{ct} **(in.)**	d_{cb} **(in.)**	R_{fe} **(kips)**	R_{re} **(kips)**	R_{de} **(kips)**	$\frac{R_{fe}}{R_{re}}$	$\frac{R_{fe}}{R_{de}}$
31	15.4	30.7	3.24	3.24	14.1	14.7	13.6	0.959	1.04
33	15.4	30.7	1.71	1.71	21.3	21.1	20.3	1.01	1.05
35	15.4	30.7	1.71	3.24	18.5	18.5	17.8	1.00	1.04
37	15.4	30.7	3.24	1.71	16.5	17.1	15.8	0.962	1.04
39	7.68	15.4	3.24	3.24	42.8	45.1	41.7	0.948	1.03
41	7.68	15.4	1.71	1.71	72.6	65.0	62.4	1.12	1.16
43	7.68	15.4	1.71	3.24	64.4	56.9	54.6	1.13	1.18
45	7.68	15.4	3.24	1.71	48.7	52.6	48.6	0.926	1.00
47	7.68	30.7	3.24	3.24	40.3	41.7	41.7	0.967	0.967
49	7.68	30.7	1.71	1.71	68.3	60.0	62.4	1.14	1.09
51	7.68	30.7	1.71	3.24	61.3	52.5	54.6	1.17	1.12
53	7.68	30.7	3.24	1.71	45.5	48.6	48.6	0.936	0.936
							Average	1.02	1.05
							Standard Deviation	0.0902	0.0736

R_{fe} = critical reaction from finite element model
R_{re} = critical reaction with C_b calculated with the original regression equation
R_{de} = critical reaction with C_b calculated with the simplified design equation